2011 IEEE International Conference on Robotics and Automation
Shanghai International Conference Center
May 9-13, 2011, Shanghai, China

Modeling and Implementation of Nanoscale Robotic Grasping

Hui Xie, *Member, IEEE,* Pierre Lambert, and Stéphane Régnier

***Abstract*—To understand robotic grasping at the nanoscale, contact mechanics between nano grippers and nano samples was studied. Contact mechanics models were introduced to simulate elastic contacts between various profiles of flat surface, sphere and cylinder for different types of nano samples and nano grippers. Analyses and evaluation instances indicate that friction forces, commonly used in macro grasping to overcome the gravity, at nanoscale is often not enough to overcome relatively strong adhesion forces to pick up the nano sample deposited on a substrate due to tiny contact area of the grasping. Two-finger grippers are proposed for the stable nanoscale grasping and a nonparallel gripper with a 'V' configuration was demonstrated with better grasping capabilities than a parallel one. To achieve the robotic nanoscale grasping, a nano gripper constructed from two individually actuated and sensed tips is presented. Pick-and-place manipulation of silicon nanowires validate the theoretical analyses and capabilities of the proposed nano gripper.**

I. Introduction

Grasping has been widely used to move an object from one place to another for macro robotic manipulation and assembly. In the past decade, research efforts have been made to scale down the robotic grasping to microscale with micro grippers for integrating functional micro components into mechatronics systems or performing scientific explorations in biology [1–4]. Recent work has been reported that pick-and-place manipulation at several micrometers has been achieved with a dual-tip gripper [5]. Some basic problems in micromanipulation attributed to the scale effect [6], such as suitable grasping principles and release techniques taking into account of adhesion forces, have been identified, thereby providing some references for the nanoscale grasping. However, the scale effects become more severe when the manipulation size decreases to nanoscale. In this case, strong sticking phenomena and very tiny size of a nano object to be grasped put forward higher requirements for grasping schemes and fabricating techniques of nano grippers.

In the past two decades, nanomanipulation were generally restricted to 2D nano patterns building or in-plane nano material characterization through pushing/pulling operations on a single surface using atomic force microscopes (AFM) [7–10], although nano samples have been manipulated, assembled and characterized by nanorobots equipped with manipulators or grippers in scanning electron microscopes (SEM) and transmission electron microscopes (TEM) [11], [12] due to the vacuum environment and the visual feedback. Liquid medium, where the adhesion forces are greatly reduced, also enables noncontact grasping with optical [13] and magnetic tweezers [14]. In order to fabricate smart nano grippers, carbon nanotubes (CNT) have been used as self-actuated gripper fingers [15], [16]. However, the alignment of CNT fingers remains a challenge, and grasping capabilities of the CNT grippers need further tests, especially tasks confined in ambient conditions with presence of strong adhesion forces.

To achieve the robotic nanoscale grasping, the main difficulties are fabricating very sharp end-effectors with a size comparable to the nano object to be grasped and with enough grasping force output to overcome strong adhesion forces, as well as capabilities of force sensing while controlling interactions between the nano object and the end-effectors or the substrate. For macroscopic, even for microscopic applications, friction forces between a gripper and the objects can be generally strong enough for stable grasping operations. However, frictional grasping does not work in this case since contact-induced friction forces are often less than relatively large adhesion forces due to small contact areas that are favorable to nano object release.

In order to understand physical interactions during mechanical nanoscale grasping, based on the Hertz [17] and some other extended theroies, various contact profiles among flat surface, sphere and cylinder for different types of grippers and nano samples are analyzed. Grasping capabilities of nano grippers with two-finger configuration are discussed. As an example, we present a prototype of two-tip AFM system, of which two collaborative cantilevers with protruding tips are used to form a nanotip gripper. In our approach, interactions between the nano gripper and the nano object during the grasping are analyzed and simulated. We have used the developed nanotip gripper to build a 3-D nanowire crossbar.

II. Problem Definition

A. Challenges

Modeling and simulation of contact mechanics between the nano object, gripper and a substrate is required for understanding interactions of the nanoscale grasping, thereby providing theoretical estimation of grasping forces, releasing adhesion forces and maximum contact stress for reliable pickup and smooth release operations, as well as protecting the both of the gripper and the nano object from damage. Thus, research on the following aspects associated with the nanoscale grasping should be addressed: (1) Estimate adhesion Forces of the contacting surfaces. (2) Compute nanoscale friction at a interfacial surface. (3) Calculate maximum contact stress on the contact area. (4) Develop grasping and release schemes according to simulation and analyses of the nanoscale contact.

This work was supported in part by the ANR (French Research Agency) through the NANOROL Project under ANR Grant No. PSIROB07-184846.

Hui Xie and Stéphane Régnier are with the Institut des Systèmes Intelligents et Robotique (ISIR), Université Pierre et Marie Curie/CNRS UMR7222, BC 173, 4 Place Jussieu, F-75005 Paris, France. (e-mail: xie@isir.upmc.fr, stephane.regnier@upmc.fr).

Pierre Lambert is with Université libre de Bruxelles, BEAMS department CP 165/56, 50 avenue F.D. Roosevelt, B-1050 Bruxelles, Belgium. (e-mail: pierre.lambert@ulb.ac.be).

B. Contact Configurations

Fig. 1 shows four configurations of the nanoscale grasping using two-finger grippers with cylindrical and rectangular fingers. Each is used for nanowire/tube or nanoparticle (sphere). Hence possible contact states between the gripper and the nano object being grasped can be classified as:

1) Contact between two cylinders (C-C). As seen in Fig. 1 (a), a nanowire/tube is grasped by cylindrical fingers.
2) Contact between a cylinder and a sphere (C-S). As seen in Fig. 1 (b), e.g., a nanoparticle is grasped by a cylindrical fingers.
3) Contact between a flat surface and a cylinder (FS-C) contact. Fig. 1(a) and (c) show FS-C contacts between a nanowire/tube and the substrate or rectangular fingers.
4) Contact between a flat surface and a sphere (FS-S). As seen in Fig. 1(b) and (d), contacts between a nanoparticle and the substrate or rectangular grippers.

III. Contact Mechanics of Nanoscale Grasping

In the general case, when two surfaces are brought into contact under a load P, within the defined frame, the separation h between the two surfaces is given by:

$$h = Ax^2 + By^2 = \frac{1}{2R_1}x^2 + \frac{1}{2R_2}y^2 \tag{1}$$

where A and B are determined by $R_1 = R_1^{'}R_1^{''}/(R_1^{'} + R_1^{''})$ and $R_2 = R_2^{'}R_2^{''}/(R_2^{'} + R_2^{''})$ the principal relative radius of curvature. $R^{'}$ and $R^{''}$ are the principal radius of each contact surface at the origin. An equivalent radius $R_e = \frac{1}{2}(AB)^{-\frac{1}{2}}$.

Assuming the contact area is elliptical in shape and with semi-axis a and b, we obtain [17]:

$$\begin{cases} A = \frac{p_0 b a^2}{E^* e^2}\left[\mathbf{K}(e) - \mathbf{E}(e)\right], \\ B = \frac{p_0 b a^2}{E^* e^2}\left[\frac{a^2}{b^2}\mathbf{E}(e) - \mathbf{K}(e)\right], \end{cases} \tag{2}$$

where $\mathbf{K}$(e) and $\mathbf{E}$(e) are complete elliptic integrals of argument $e = (1 - b^2/a^2)^{1/2}, b < a$. E^* is the elastic constants and p_0 is the maximum pressure on the contact area. From (2), S can be calculated from:

$$S = \pi ab = \pi\left(\frac{3PR_e}{4E^*}\right)^{\frac{2}{3}}\left[F_1(e)\right]^2 \tag{3}$$

where $F_1(e) = \frac{4}{\pi e^2}(\frac{b}{a})^{\frac{3}{2}}\left\{\left[(\frac{a}{b})^2\mathbf{E}(e) - \mathbf{K}(e)\right]\left[\mathbf{K}(e) - \mathrm{E}(e)\right]\right\}^{\frac{1}{2}}$. The maximum contact pressure p_0 is given by:

$$p_0 = \frac{3P}{2\pi ab} = \left(\frac{6PE^{*2}}{\pi^3 R_e^2}\right)^{\frac{1}{3}}\left[F_1(e)\right]^{-2}. \tag{4}$$

A. Mechanics of C-C Contact

As two cylinders are brought into contact, e.g., a gripper with cylindrical fingers is used to grasp nanowires, we may put $R_1^{'} = R_f$ and $R_1^{''} = \infty$ for the gripper $R_2^{'} = \infty$ and $R_2^{''} = R_w$ in (1), here, R_f and R_w are the radius of the gripper finger and nanowire at contact locations. A and B will be calculated by (2), which in turn S and p_0 respectively through (3) and (4).

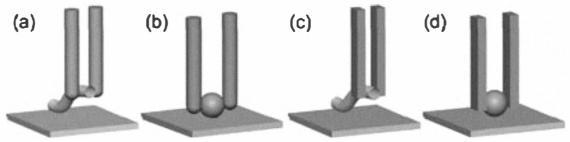

Fig. 1. (a), (c), the nanowire/tube is by rectangular and cylindrical gripper, respectively. (b), (d), the nanoparticle is grasped by rectangular and cylindrical fingers, respectively.

Adhesion forces on the C-C contact can be estimated as the "pull-off" force between two cylinders by [18]:

$$F_s = \frac{4\pi R\Delta\gamma}{\sin\psi}, \tag{5}$$

where $\Delta\gamma$ is the work of adhesion, ψ is angle that the cylinder axes inclined to each other and $R = \frac{R_f R_c}{R_f + R_c}$.

B. Mechanics of C-S Contact

As a spherical nano object (with a radius R_s) and a cylindrical gripper are brought into contact, From (5), if we set $\psi = 90°$ and $R = \frac{R_f R_s}{2R_f + R_s}$, an approximate adhesion force of C-S contact is obtained:

$$F_s = 4R\pi\Delta\gamma. \tag{6}$$

Similarly, contact area S and maximum pressure p_0 can be respectively calculated by substituting (6) into (3) and (4).

C. Mechanics of FS-C Contact

Adhesive contact between a flat surface and a cylinder (FS-C) has been studied with a JKR model [19].

$$\frac{P + F_s}{l} = \frac{\pi E^* a^2}{4R} + \sqrt{2\pi E^* a\Delta\gamma} \tag{7}$$

where l is the length of the cylinder, a is the half-width of the contact and the JKR pull-force F_s for line contact is [20]:

$$F_s = \frac{3}{2}l\left(4\pi E^* R\Delta\gamma^2\right)^{1/3} \tag{8}$$

Thus, from (7) and (8), a half-width a can be calculated and then contact area $S = 2al$ and $p_0 = \frac{3}{2}\frac{P + F_s}{S}$.

D. Mechanics of FS-S Contact

While a sphere on a flat surface, the contact area is approximately given by the JKR [19] (lower boundary) or DMT (higher boundary) models. According to the Maugis parameter $\lambda = \delta_0\left(R/\Delta\gamma E^{*2}\right)^{\frac{1}{3}}$ (δ_0 is limiting surface stress) [21]:

$$\lambda < 0.1 \Rightarrow \mathrm{DMT} \quad S = \pi\left[\frac{R}{K}(P + 2\pi R_s\Delta\gamma)\right]^{\frac{2}{3}} \tag{9}$$

$$\lambda \in (0.1, 5) \Rightarrow \mathrm{Dugdale}\ \ S = \pi m_0^2\left(\frac{\alpha + \sqrt{1 + \frac{P}{F_s}}}{1 + \alpha}\right)^{\frac{4}{3}} \tag{10}$$

$$\lambda > 5 \Rightarrow \mathrm{JKR} \quad S = \pi a_{\mathrm{JKR}}^2 \tag{11}$$

where $a_{\mathrm{JKR}} = \left[\frac{R_s}{K}\left(P + 3\pi R_s\Delta\gamma + \sqrt{6\pi R_s\Delta\gamma P + (3\pi R_s\Delta\gamma)^2}\right)\right]^{\frac{1}{3}}$ and $K = \frac{4}{3}\left(\frac{1-\nu_1^2}{E_1} + \frac{1-\nu_2^2}{E_2}\right)^{-1}$ is the reduced elastic modulus for the contact interface, in which ν_1 and ν_2 are the Poisson's ratios, and E_1 and E_2 are the Young's modulus of each contact part. m_0 can be calculated by:

$$m_0 = \left(1.54 + 0.279\frac{2.28\lambda^{\frac{1}{3}} - 1}{2.28\lambda^{\frac{1}{3}} + 1}\right)\left(\frac{\pi\Delta\gamma R_s^2}{K}\right)^{\frac{1}{3}} \quad (12)$$

where α can be calculated from: $\lambda = -0.924\ln(1 - 1.02\alpha)$, and F_s for Dugdale theory can be given by:

$$F_s = \pi\left(\frac{7}{4} - \frac{1}{4}\frac{4.04\lambda^{1/4} - 1}{4.04\lambda^{1/4} + 1}\right)R_s\Delta\gamma \quad (13)$$

E. Friction Forces at the Contact Interface

The well-known Amontons' law shows that the friction force F_f is proportional to a normal force applied on two contacting surfaces with many asperities. However, as the contact area is reduced to the nanoscale, the friction with a single asperity contact is more suitably described by [22]:

$$F_f = \tau S \quad (14)$$

where τ is a effective friction coefficient, and S is the contact area that is associated with the sum of the external force and the adhesion force on the contact area. τ can be estimated as $\tau \approx 0.0345G^*$ [23], where $G^* = \left(\frac{2-\nu_1}{G_1} + \frac{2-\nu_2}{G_2}\right)^{-1}$, ν and G are the Poisson's ratio value and shear strength of each of contacting surfaces, respectively.

IV. Nanoscale Grasping with Two-Finger Grippers

Grippers with two fingers are widely proposed in micro/nano applications. Fig. 2 shows nanoscale grasping with two-finger grippers. Two configurations of the grippers with parallel- and nonparallel-finger are considered.

A. Grasping with the Two-Finger Gripper

1) Parallel Fingers: Fig. 2 (a) shows a gripper formed by two parallel fingers with a tip radius r. To vertically pick up the nano object with a radius of R, the following inequalities should hold:

$$R > r \quad \text{and} \quad {}^tF_f^{\max} > \frac{1}{2}{}^sF_a. \quad (15)$$

During grasping, ${}^tF_f$ can be adjusted by increasing or decreasing ${}^tF_p$ by driving single or dual fingers, overcoming the adhesion force ${}^sF_a$. Similarly, for a stable vertical release of the nano object, the grasping force can be reduced to generate a certain value ${}^tF_f^0$ that makes the nano object easily sticky to the substrate with the following inequalities:

$${}^tF_f^0 < \frac{1}{2}{}^sF_a \quad \text{and} \quad {}^tF_f^0 \geq {}^tF_f^{\mathrm{ad}}, \quad (16)$$

where ${}^tF_f^{\mathrm{ad}}$ is the adhesive friction force derived from ${}^tF_a$ without any external clamping forces.

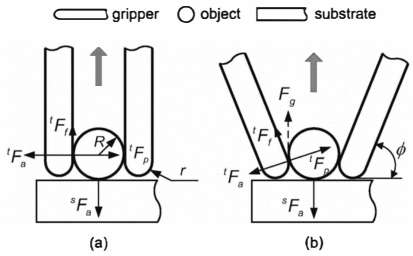

Fig. 2. Nanoscale grasping with two-finger grippers. (a) The gripper with parallel fingers. (b) The nonparallel gripper with a "V" configuration.

TABLE I
INTERRACIAL CONTACT PARAMETERS OF MATERIALS

		Silicon	SiO_2	Gold
Surface energy J/m^2	γ	1.4	0.16	1.5
Young's modulus (GPa)	E	160	73	79.5
Poisson's ratio	ν	0.17	0.165	0.42

MEMS grippers have been demonstrated to pick up vertically aligned carbon nanotube in the SEM [14], [24]. However, this type of MEMS grippers might meet difficulties in grasping nanotubes attached horizontally to a substrate due to it dull end, as well as small gripper-nanotube contact area which cannot provide a sufficient grasping force (friction forces).

2) Nonparallel Fingers: To increase the grasping capability, fingers aligned with a "V" configuration is proposed in Fig. 2(b). Similar with the parallel fingers, the following inequalities should hold to pick up the nano object:

$$R > r \quad \text{and} \quad F_g = ({}^tF_f^{\max}\cos\phi + {}^tF_p\sin\phi) > \frac{1}{2}{}^sF_a. \quad (17)$$

Obviously, the tilted angle ϕ makes the grasping stronger due to a contribution of clamping forces ${}^tF_p$, compounding with the friction forces ${}^tF_f$ to overcome the adhesion forces ${}^sF_a$.

To compare the grasping capabilities of the parallel- and nonparallel-finger gripper, an example of nanowire grasping with a cylindrical gripper is simulated. The nanowire is horizontally deposited on a substrate and vertical grasp makes an orthogonal contact between the gripper and the nanowire. Supposing the gripper and the nanowire are made up of silicon with SiO_2 coating and with the same radius of 50 nm, ${}^tF_a$ and ${}^tF_f$ can be respectively estimated by (5) and (14) with parameters described in Table I.

The simulated grasping force F_g is plotted in Fig. 3 as a function of the angle ϕ and the clamping force ${}^tF_p$. The result shows that the fingers with larger tilted angle intends to produce greater grasping force, e. g., with a same clamping force ${}^tF_p = 100$ nN, the nonparallel gripper with tilted angle $\phi = 70°$ produces more 1.5 times of grasping force than that of the parallel gripper.

3) Release Schemes: The release operation of the two-finger gripper is more complicated, especially rectangular fingers, which produce comparable adhesion forces of the finger-nano object contact to the substrate-nano object contact. In contrast, cylindrical fingers produce smaller adhesion forces, resulting in easier release operations.

As shown in Fig. 4(a), in the first step of release, the right finger separate from the nano object. In this case, two opposing

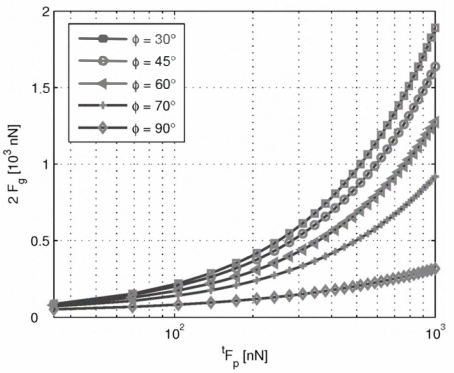

Fig. 3. Simulated grasping forces F_g with different clamping angles

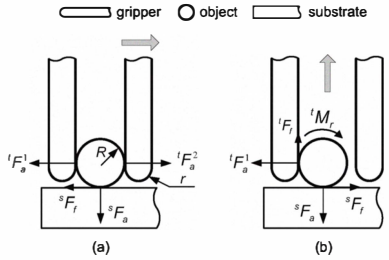

Fig. 4. (a) Horizontally open the right finger. (b) Vertical release.

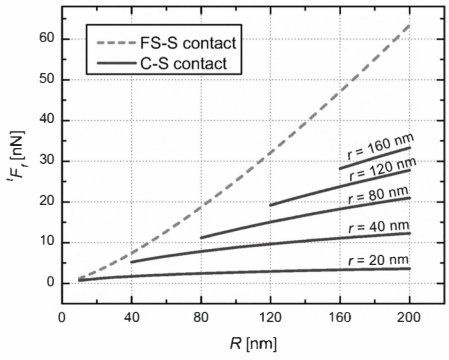

Fig. 5. Simulated ${}^tF_f$ of the rectangular and the cylindrical grippers.

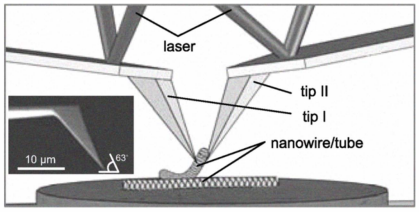

Fig. 6. Nonparallel configuration of the nanotip gripper. The inset shows a SEM side view of the AFM tip.

adhesion forces from the fingers are canceled out each other and the friction force ${}^sF_f$ is used to hold the nano object. When the right finger has been separated from the nano object, the gripper move upward in Fig. 4(b) for release operation with conditions: ${}^tF_f < {}^sF_a$. Note that in this last step, the nano object might be rolled slightly due to ${}^tM_r$ derived from ${}^tF_f$. However, apart from the releasing accuracy, this scheme may be effective for release operation of the two-finger gripper.

An example of grasping a gold nanoparticle $R = 50$ nm deposited on a Si substrate with a silicon rectangular gripper is presented. We can calculate ${}^sF_a = {}^tF_a = 243$ nN using (13) ($\lambda = 3.38$) and adhesive friction forces ${}^sF_f = {}^tF_f = 84$ nN using (14) with corresponding parameters described in Table I. The calculated results show that the gold nanoparticle can be successively released by the rectangular gripper in air. We can infer from this that nanowire release using this scheme is easier than nanoparticle release because of the much stronger adhesion force of the nanowire-substrate contact.

Although theoretical calculation verifies that the rectangular gripper can release the nanoparticle, the comparable magnitude of ${}^sF_a$ and ${}^tF_f$ brings uncertainties to the releasing process. From (14), simulated ${}^tF_f$ with the rectangular and cylindrical silicon grippers are plotted in Fig. 5 as a function of the gold nanoparticle sizes. It shows that ${}^tF_f$ will be greatly reduced with a cylindrical finger under the same conditions. ${}^tF_f$ can be further reduced with thinner cylindrical grippers.

V. Experimental Implementation with a Nanotip Gripper

A. Setup of the Nanotip Gripper

Fig. 6 shows the setup of a nanotip gripper that is comprised of two AFM cantilevers (ATEC-FM Nanosensors) with protruding tips (see the inset). Normal stiffness k_b^n of the cantilevers and optical lever sensitivities S_n are shown in Table II. Detailed descriptions of the system setup and grasping protocols can be seen in [25].

Nanoscale grasping with the proposed gripper benefits from followings: (1) The AFM tip is very tiny (typically with an apex radius of 10 nm or less) with respect to the size of the nano object to be manipulated, leading to smaller adhesive forces that is favorable to releasing operation. (2) The tetrahedral (tapered shape close to the very end) tip of the cantilever reduces contacting adhesion forces. In addition, the tip is tiled 63° that can be used to make a "V" configuration that provides larger grasping force. (3) More importantly, the gripper can be used as a normal AFM to image the nano object, as well as locate the fingers for gripper alignment. It makes possible to fulfill nanoscale grasping without visual feedback (normally SEM or TEM vision) in the ambient conditions.

B. Mechanic Analysis of the Grasping

Fig. 7 shows a mechanic analysis of a cantilever used as a gripper finger. In experiments, cantilever's dimensions of beam length L, beam width w and tip height l are measured under an optical microscope. The beam thickness t is determined using forced oscillation method [26].

When a force F is applied on the end of the tip, displacements δ_x, δ_y and δ_z depend on the stiffness of cantilever on

TABLE II
Cantilevers Stiffness and Optical Lever Sensitivities

Parameters	Cantilever I	Cantilever II
k_b^n	2.72 N/m	2.78 N/m
S_n	0.51 μm/V	0.49 μm/V

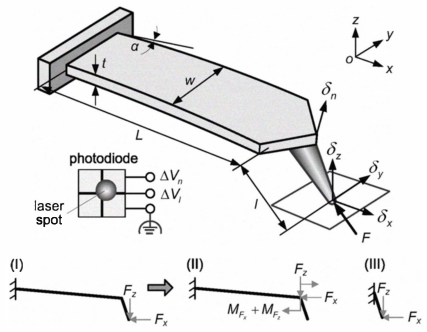

Fig. 7. Mechanics analysis of a AFM cantilever during grasping operation.

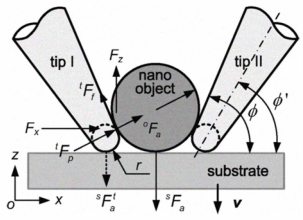

Fig. 8. Force simulation using the nonparallel two-tip gripper

each axis in the defined fame. As seen in inset (I)–(III) of Fig. 7, decoupling displacement on each axis is calculated by:

$$\begin{bmatrix} \delta_x \\ \delta_z \end{bmatrix} = \begin{bmatrix} \sin\alpha & \sin\phi' & l\sin\phi' \\ \cos\alpha & \cos\phi' & l\cos\phi' \end{bmatrix} \begin{bmatrix} d_b^{F_x} + d_b^{F_z} \\ d_t^{F_x} + d_t^{F_z} \\ \theta_b^{F_x} + \theta_b^{F_z} \end{bmatrix}, \quad (18)$$

where $\phi' = 60°$ is the tilted angle through the rotation axis of the tip relative to the substrate (seen in Fig. 8), α is the mounting angle of the cantilever, θ is the angular deflection of the beam and d is deflection of cantilever's beam and tip (respectively labeled by subscripts b and t with superscripts of force F_x and F_z). The calculation of the deflections is shown as follows: $d_b^{F_x} = \frac{F_x}{k_b^n}\left(\sin\alpha + \frac{3l\sin\phi'}{2L}\right)$, $d_b^{F_z} = \frac{F_z}{k_b^n}\left(\cos\alpha + \frac{3l\cos\phi'}{2L}\right)$, $d_t^{F_x} = \frac{F_x\sin\phi'}{k_t}$, $d_t^{F_z} = \frac{F_z\cos\phi'}{k_t}$, $\theta_b^{F_x} = \frac{3F_x}{k_b^n L}\left(\frac{\sin\alpha}{2} + \frac{l\sin\phi'}{L}\right)$, $\theta_b^{F_z} = \frac{3F_z}{k_b^n L}\left(\frac{\cos\alpha}{2} + \frac{l\cos\phi'}{L}\right)$.

C. Grasping Capabilities

1) Grasping Force: Fig. 8 shows a force simulation for nanowire grasp using the proposed nanotip. Equations can be obtained for a static equilibrium:

$$\begin{cases} F_z = ({}^tF_f\sin\phi + {}^tF_p\cos\phi) = \frac{1}{2}{}^sF_a \\ F_x = ({}^tF_p\sin\phi - {}^tF_f\cos\phi) \end{cases} \quad (19)$$

where $\phi = 68°$. ${}^tF_f$ can be calculated by:

$${}^tF_f = \tau\pi\left[\frac{3({}^tF_p + {}^tF_a)R_e}{4E^*}\right]^{2/3}[F_1(e)]^2, \quad (20)$$

where ${}^tF_a = {}^oF_a$ is the adhesion force estimated by (5). to avoid damage on both the gripper or the nanowire.

The normal force F_z applied on the end of the tip can be calculated from voltage output ΔV_n of optical levers by:

$$k_b^n\delta_n = k_b^n(d_b^{F_x} + d_b^{F_z}) = \Delta V_n S_n, \quad (21)$$

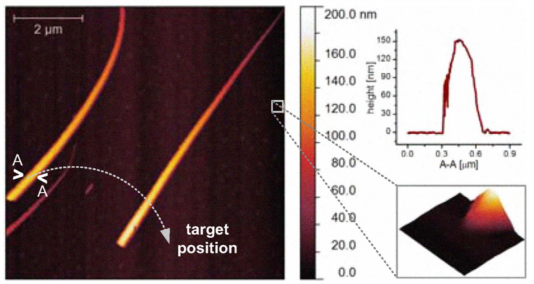

Fig. 9. Pre-scanned image of the SiNW. Insets show a 3D topographic image of the tip II and the nanowire height at location A–A.

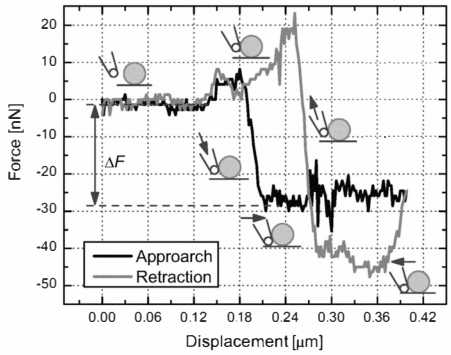

Fig. 10. Contact detection by the normal force sensing on tip II.

where δ_n is the normal deflection of the cantilever beam, S_n is the normal sensitivity of the optical lever.

2) Task Description: In experiments, silicon nanowires (SiNWs) were deposited on a freshly cleaned silicon wafer coated with 300 nm silicon dioxide. A pre-scanned image (8 μm × 8 μm) is shown in Fig. 9, which includes the topographic image of SiNWs and a local image of tip II (inset). When the left SiNW is successfully grasped at location A–A, it will be transported to the target position and released on the right SiNW to build a nano crossbar.

3) Grasping Detection: Fig. 10 shows an example of the grasping detection with tip II: As seen icons in the graph, the tip starts to dig into the root of the SiNW as the tip contacts with the SiNW. Further move leads to unobvious change of voltage output. During the retraction, after the contact breaks with the substrate, the bending force sharply reaches a positive peak. When the tip digs into the SiNW, the cantilever produces a pre-grasping force $\Delta F = 27$ nN with a voltage difference of about 20 mV. The corresponding preload on the tip II is estimated as ${}^tF_p = 26$ nN using (19).

4) Force Sensing during Pick-and-Place: Fig. 11 shows an example of the peeling force spectroscopy on one of the tips during pick-and-place of the same SiNW. The curve starts from contact state. As the SiNW was picked up, the cantilever is bent downward until the cantilever pulls off the substrate with a voltage difference of 75 mV that indicates a pull-off force $\Delta F_1 = 103$ nN. As the gripper is moved up further, the force magnitude keeps slightly increasing. Snap-in occurs during the retraction at 25 nm after a mild force decrease.

During the pickup, the maximum peeling force occurs at the start of the retraction, where the voltage is about -105

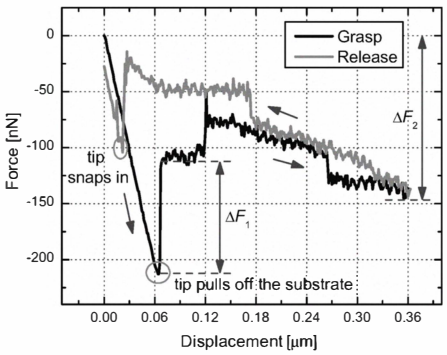

Fig. 11. Force detection on one of the tips during the grasping and releasing operation.

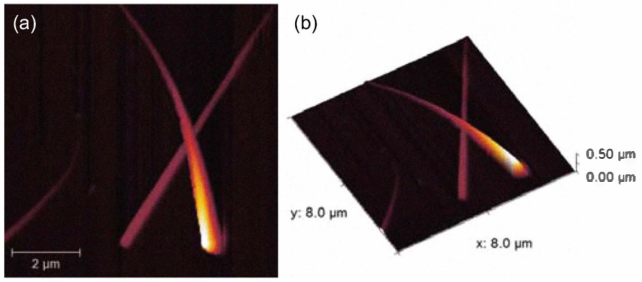

Fig. 12. (a) A post-manipulation image verifies a SiNW crossbar. (b) 3D topographic image of the SiNW crossbar.

mV that indicates a grasping force of $\Delta F_2 = 144$ nN. At this point, ${}^tF_p = 218$ nN and a maximum contact stress $p_0 = 7.1$ Gpa are calculated with $R \approx 19.5$ nm at contact location of 55 nm from the end of the tip. Fortunately, this contact stress is still below the yield stress of the silicon on the nanoscale contact (around $12 \sim 13$ GPa) due to size effects [22].

5) Pick-and-Place Result: A post-manipulation image in Fig. 12 verifies that the SiNW has been successfully transported and piled onto another SiNW, building a nano crossbar. During the pick-and-place, once the SiNW was reliably grasped, the gripper moved up 800 nm with a velocity of 80 nm/s, then the SiNW was transported a distance of 4.05 μm on the X-axis with a velocity of 150 nm/s and 1.95 μm on the Y-axis with a velocity of 72 nm/s.

VI. Conclusion

It is well known that the nanoscale robotic grasping is still a challenge. For understanding the interactive phenomena between a gripper and a nano object, contact mechanics were modeled for different contacting surfaces. With the contact modeling, interfacial adhesion forces, contact deduced friction forces and contact stress could be easily estimated, thereby providing theoretical analysis for the gripper design and task planning for a successful nanoscale grasping. Analysis shows that the gripper with a nonparallel configuration has better grasping capabilities than the parallel configuration. A homemade gripper constructed from two AFM cantilevers with a 'V' configuration was introduced. Its grasping capabilities were analyzed in detail. Subsequently, a successful pick-and-place manipulation of silicon nanowires was performed.

References

[1] W. Driesen, T. Varidel, S. Régnier, and J, M. Breguet, "Micromanipulation by adhesion with two collaborating mobile micro robots," *J. Micromech. Microeng.*, vol. 15, no. 10, pp. S259–S267, 2005.

[2] H. Xie, W. B. Rong, and L. N. Sun, "A flexible experimental system for complex microassembly under microscale force and vision-based control," *Int. J. Optomechatro.*, vol. 1, no.1, pp. 80–102, 2007.

[3] B. L. Walle, M. Gauthier, and N. Chaillet, "Principle of a submerged freeze gripper for microassembly," *IEEE Trans. Robot.*, vol. 24, no. 4, pp. 897–902, 2008.

[4] K. Y. Kim, X. Y. Liu, Y. Zhang, and Y. Sun, "Nanonewton force-controlled manipulation of biological cells using a monolithic MEMS microgripper with two-axis force feedback," *J. Micromech. Microeng.*, vol. 18, no. 5, pp. 055013, 2008.

[5] H. Xie, and S. Régnier, "Three-dimensional automated micromanipulation using a nanotip gripper with multi-feedback," *J. Micromech. Microeng.*, vol. 19, pp. 075009, 2009.

[6] A. Menciassi, A. Eisinberg, I. Izzo, and P. Dario, "From 'macro' to 'micro' manipulation: models and experiments," *IEEE/ASME Trans. Mechatro.*, vol. 9, no. 2, pp. 311–320, 2004.

[7] M. R. Falvo, R. M. I. Taylor, A. Helser, V. Chi, F. P. J. Brooks, S. Washburn, and R. Superfine, "Nanometre-scale rolling and sliding of carbon nanotubes," *Nature*, vol. 397, pp. 236–238, 1999.

[8] R. Resch, D. Lewis, S. Meltzer, N. Montoya, B. E. Koel, A. Madhukar, A. A. G. Requicha, and P. Will, "Manipulation of gold nanoparticles in liquid environments using scanning force microscopy," *Ultramicroscopy*, vol. 82, pp. 135–139, 2000.

[9] M. Sitti, "Atomic force microscope probe based controlled pushing for nanotribological characterization," *IEEE/ASME Trans. Mechatron.*, vol. 9, no. 2, pp. 343–349, 2004.

[10] H. Chen, N. Xi, and G. Y. Li, "CAD guided automated nanoassembly using automic force microscopy-based nanorobotics," *IEEE Trans. Auto. Sci. Eng.*, vol. 3, no. 3, pp. 208–217, 2006.

[11] T. Fukuda, F. Arai, and L. X. Dong, "Assembly of nanodevices with carbon nanotubes through nanorobotic manipulations," *Proc. IEEE*, vol. 91, no. 11, pp. 1803–1818, 2003.

[12] K. N. Andersen, D. H. Petersen, K. Carlson, K. Mølhave, O. Sardan, A. Horsewell, V. Eichhorn, S. Fatikow and P. Bøggild, "Multimodal electrothermal silicon microgrippers for nanotube manipulation," *IEEE Trans. Nanotech.*, vol. 8, no. 1, pp. 76–85, 2009.

[13] L. Bosanac, T. Aabo, P. M. Bendix, and L. B. Oddershede, "Efficient optical trapping and visualization of silver nanoparticles," *Nano letters*, vol. 8, no.5, 1486–1491, 2008.

[14] A. H. B. de Vries, B. E. Krenn, R. van Driel, and J. S. Kanger, "Micro magnetic tweezers for nanomanipulation inside live cells," *Biophysical J*, vol. 88, no.3, pp. 2137–2144, 2005.

[15] P. Kim, and C. M. Lieber, "Nanotube nanotweezers," *Science*, vol. 286, no. 5447, pp. 2148–2150, 1999.

[16] J. E. Jang, S. N. Cha, Y. Choi, D. J. Kang, D. G. Hasko, J. E. Jung, J. M. Kim, and G. A. J. Amaratunga, "A nanogripper employing aligned multiwall carbon nanotubes," *IEEE Trans. Nanotech.*, vol. 7, no. 4, pp. 389–393, 2008.

[17] H. Hertz, "On the contact of elastic solids," *J. Reine Angew. Math.*, vol. 92, pp. 156–171, 1881.

[18] J. N. Israelachvili, *Intermolecular and surface forces*, New York: Academic, 1992.

[19] M. K. Chaudhurya, T. Weaver, C. Y. Hui, and E. J. Kramer, "Adhesive contact of cylindrical lens and a flat sheet," *J. Appl. Phys.*, vol. 80, no.1 pp. 30–37, 1996.

[20] K. L. Johnson and J. A. Greenwood, "A Maugis analysis of adhesive line contact," *J. Phys. D: Appl. Phys.*, vol. 41, pp. 155315, 2008.

[21] D. Maugis, "Adhesion of spheres: the JKR-DMT transitionusing a Dugdale model," *J. Colloid Interface Sci.*, vol. 150, pp. 243–269, 1992.

[22] B. Bhushan, *Springer handbook of nanotechnology*, Springer-Verlag, Heidelberg, 2004.

[23] G. Dedkov, "Friction on the nanoscale: New physical mechanisms," *Materials Letters*, vol. 38, pp. 360–366, 1999.

[24] K. Molhave, T. Wich, A. Kortschack and P. Boggild, "Pick-and-place nanomanipulation using microfabricated grippers," *Nanotechnology*, vol. 17, pp. 2434–2441, 2006.

[25] H. Xie, D. S. Haliyo, and S. Régnier, "A versatile atomic force microscope for three-dimensional nanomanipulation and nanoassembly," *Nanotechnology*, vol. 20, pp. 215301, 2009.

[26] H. Xie, J. Vitard, D. S. Haliyo, and S. Régnier, "Enhanced accuracy of force application for AFM nanomanipulation using nonlinear calibration of optical levers," *IEEE Sensor J.*, vol. 8, no. 8, pp. 1478–1485, 2008.